4–6 December 2023

LATIN AMERICA UNCONVENTIONAL RESOURCES TECHNOLOGY CONFERENCE
FUELED BY SPE • AAPG • SEG

Buenos Aires, Argentina

Latin America URTeC: 3969293

Sensitivity analysis of the main variables affecting the EUR response under parent-child effect, using a comprehensive simulation workflow in the Core of Vaca Muerta

David Martins Cruz*[1], Mauro Iván Weimann[2], Dave Ratcliff[3], 1. Iberam, 2. YPF, 3. ResFrac.

Abstract

The topic of this paper is related to the study of what is known in the industry as the "parent-child" effect. This is accomplished by using a coupled hydraulic fracture and reservoir simulator to perform a sensitivity analysis of the impact on the results of the EUR of the child well, based on a conceptual static model for the hub core of the Vaca Muerta, considering two landing zones, different spacing between wells, degree of depletion of the parent well, the addition of a second child well and the use of an improved completion design for the child well. The objective is to investigate, through sensitivity analysis, the scenarios with the greatest impact on the EUR of the child well and to measure the magnitude or influence of each of them.

Once the dynamic simulation model is calibrated, the first step is to locate and stimulate a fictitious child well in the vicinity of its parent well and perform various sensitivity analyses by varying one variable while holding the other variables constant. We considered two key variables: the well spacing (200m, 300m, 400m and 600m) and the time lag between the start of production of the child well and its parent well, with depletion intervals ranging from 0 to 5 years. A second sensitivity analysis is performed by adding two child wells, 300m and 600m from the parent well, to be stimulated simultaneously using the previous time intervals. Finally, using the 300m well spacing scenario, an improved completion design for the child well was proposed and compared to the actual completion.

The result of analyzing a single child well and varying the well spacing over time intervals was, as expected, the improvement for the impairment of the child well EUR at greater distances from the depletion area, with no effect observed for the 600m spacing situation. For the case of two child wells analysis, the EUR for the outer child well at 600m showed some degree of effect (different from the previous 600m case) and for the inner child well at 300m the EUR response was similar to the single child well at 300m spacing. Finally, changing the completion design drivers (specifically volumes per cluster) of the child well showed an improvement in child well EUR reduction over the current design.

The significance of this project is to establish a workflow, or methodology, for evaluating the influence of the parent-child effect on EUR using numerical simulations that can be applied and adapted to any unconventional formation characteristics and input variables (well spacing, completion design, etc.), allowing an informed strategy definition for field development and optimized EUR. This working methodology is based on a fracture simulation software that integrates 3D reservoir model, hydraulic fracturing, and production simulations, using a single package designed to analyze the entire life cycle of a well, from fracturing to long-term production, making it suitable for the objectives of this project.

Introduction

The parent-child well problem refers to the complex and interdependent relationships that arise between wells within a field during hydraulic fracturing operations. Typically, multiple wells are drilled in close proximity, and each well undergoes independent stimulation treatments to increase productivity. However, it has been observed that subsequent wells drilled in the vicinity of previously stimulated "parent" wells often exhibit inferior performance, commonly referred to as "child" wells (Ratcliff et al., 2022). This phenomenon has generated considerable interest and concern within the oil and gas industry due to its potential negative impact on well production and project economics (Crespo et al., 2020).

Each unconventional play has its own unique set of geological, geomechanical, and reservoir characteristics. The variable heterogeneity of unconventional reservoirs and their uniqueness relative to one another make the analysis of the parent-child well phenomenon a task with a limited focus on a particular reservoir, or group of reservoirs, with similar characteristics, and to some extent based on empirical models developed from actual well data and experience from existing wells drilled in the vicinity.

This project is no exception to these challenges and is limited to the Hub Core Oil area of Vaca Muerta (Surez et al., 2016) and focusing on the reservoir properties for the T2 unit and the lower interval of the T4 unit, both landing zones shown in **Table 1** (Desjardins P. et al., 2016). Existing petrophysical, geomechanical, PVT data and production logs from actual active wells in these shales form the basis of the project´s computational modeling and calibration of the required simulations.

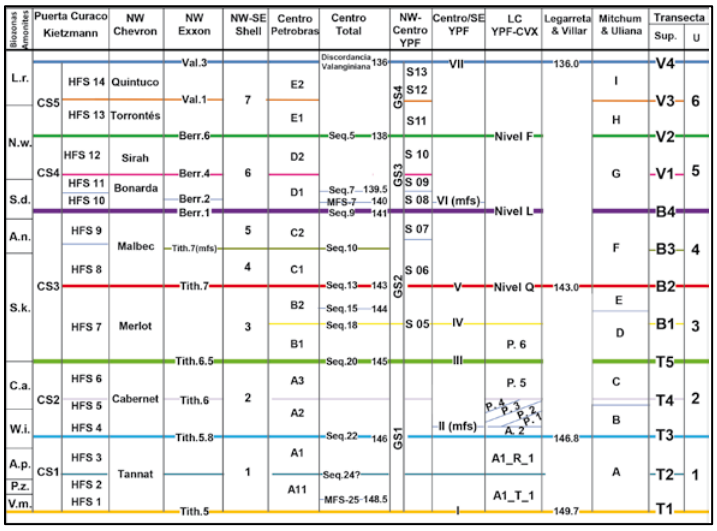

Table 1: Equivalences among stratigraphic units were presented by Desjardins P. et al., 2016, Chapter 2 of the book Transecta Regional de la Formación Vaca Muerta

The objective is to assess the parent-child well effects on the EUR over a twenty-year period of one or more child wells drilled in the vicinity of its parent well under different well spacing sensitivities and different parent well depletion intervals, considering three main scenarios: with a single child well, with two simultaneous child wells and with an improved child well completion design.

Reservoir, well and stimulation treatment data

The data received for this project includes the following data sets and will serve as the necessary input for the simulations and analysis. This data package comes from a well pad, consisting of two horizontal wells, one navigating in the lower interval of T4 landing unit (Well_2h) and the other in the T2 level (Well_3h), which will act as stand-alone or parent wells, and a vertical exploration well, Well_1v, located between the horizontal sections of these two wells, where the wireline logs were taken.

Reservoir's 3D static model

Seven variables were input into the software with log depths ranging from 2900m up to 3135m.They are used to build the 3D static model of the reservoir: porosity, permeability, Poisson´s ratio, Young´s modulus, Shmin, Sv, pore pressure, and water saturation. These variables are shown in **Figure 1**:

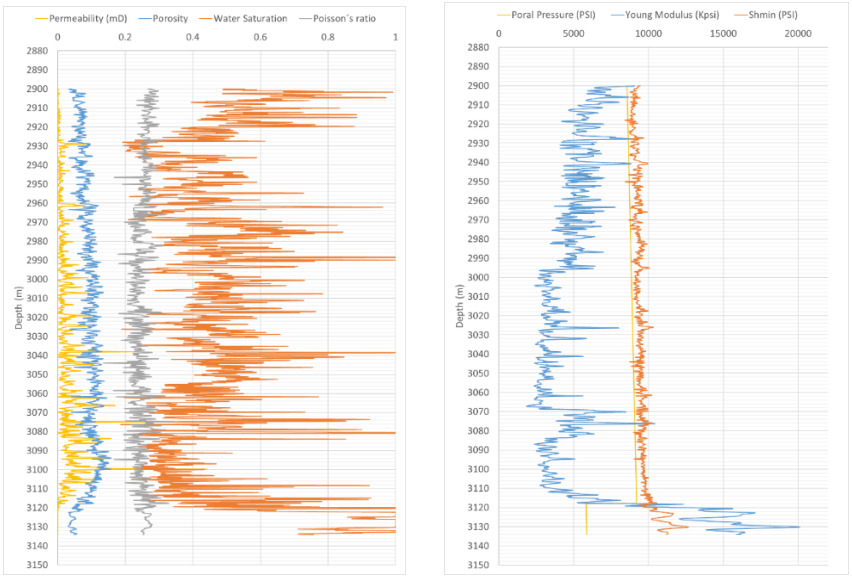

Figure 1: Logs used to simulate the reservoir 3D static model

For this study, we used a partial 3D static model, covering three stages of both wells as shown in **Figure 2**. The model has of the following dimensions: 244m in the Shmin direction, 2744m in the SHmax direction, and 235m, in the vertical axis. The static model is located approximately at the center of the horizontal sections of both wells (stages number 6, 7 and 8, in both cases) and within the vertical well which acts as the center of the cube in the Shmin and SHmax directions.

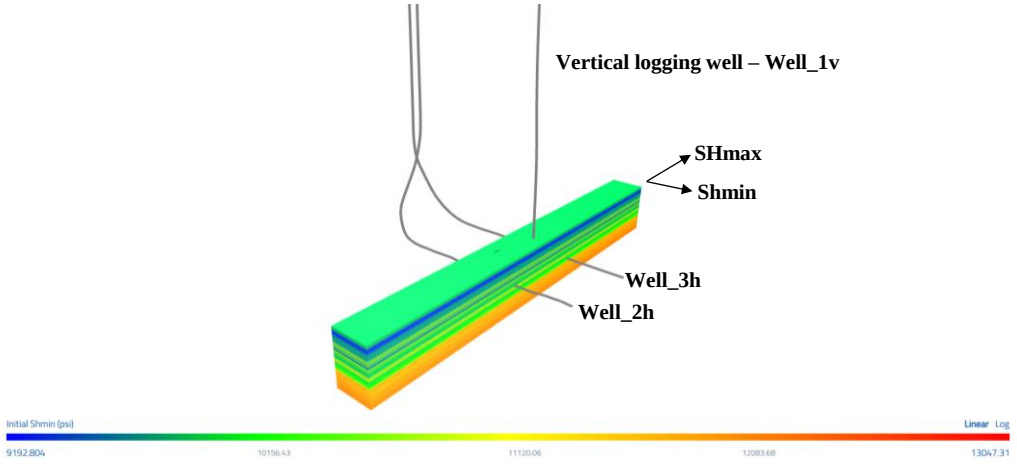

Figure 2: Visualization of the 3D static reservoir model cube

Well characteristics and completion design

Wells 2h and 3h are both monobore wells that were stimulated and later produced without tubing. The average TVD of the horizontal sections are as follows:

- Well_3h has an average TVD horizontal section of 3090m, landing in the T2 unit.
- Well_2h has an average TVD horizontal section 3043m, landing in the lower part of T4 unit.

The completion design of the horizontal section of each well is shown in **Table 2**. Stages 6, 7 and 8 were selected for the analysis due to their proximity to the vertical well, which increases the likelihood that the petrophysical and geomechanical variables logged would be consistent with what would be found in these particular intervals. A simulation of all the 15 stages would require a level of computational time and resources that would be beyond practical means, making the project infeasible.

Well_2h

Perforation name	Perf top MD (m)	Perf bottom MD (m)	Stage number	No of shots	Perf spacing (m)	Perf diameter (in)	Phasing (deg)
Perforation 48	3369.4	3370.4	15	14	26.0	0.29	60
Perforation 47	3395.4	3396.4	15	14	26.8	0.29	60
Perforation 46	3422.0	3423.0	15	14	29.9	0.29	60
Perforation 45	3452.0	3453.0	14	14	24.0	0.29	60
Perforation 44	3476.0	3477.0	14	14	24.2	0.29	60
Perforation 43	3500.0	3501.0	14	14	29.9	0.29	60
Perforation 42	3530.0	3531.0	13	14	24.0	0.29	60
Perforation 41	3554.0	3555.0	13	14	24.2	0.29	60
Perforation 40	3578.0	3579.0	13	14	29.9	0.29	60
Perforation 39	3608.0	3609.0	12	14	24.0	0.29	60
Perforation 38	3632.0	3633.0	12	14	24.2	0.29	60
Perforation 37	3656.0	3657.0	12	14	29.9	0.29	60
Perforation 36	3686.0	3687.0	11	14	24.0	0.29	60
Perforation 35	3710.0	3711.0	11	14	24.2	0.29	60
Perforation 34	3734.0	3735.0	11	14	29.9	0.29	60
Perforation 33	3764.0	3765.0	10	14	24.0	0.29	60
Perforation 32	3788.0	3789.0	10	14	24.2	0.29	60
Perforation 31	3812.0	3813.0	10	14	29.9	0.29	60
Perforation 30	3842.0	3843.0	9	14	24.0	0.29	60
Perforation 29	3866.0	3867.0	9	14	24.2	0.29	60
Perforation 28	3890.0	3891.0	9	14	29.9	0.29	60
Perforation 27	3920.0	3921.0	8	14	20.7	0.29	60
Perforation 26	3940.7	3941.7	8	14	24.2	0.29	60
Perforation 25	3964.7	3965.7	8	14	33.2	0.29	60
Perforation 24	3998.0	3999.0	7	14	24.0	0.29	60
Perforation 23	4022.0	4023.0	7	14	21.4	0.29	60
Perforation 22	4043.2	4044.2	7	14	32.7	0.29	60
Perforation 21	4076.0	4077.0	6	14	24.0	0.29	60
Perforation 20	4100.0	4101.0	6	14	24.2	0.29	60
Perforation 19	4124.0	4125.0	6	14	29.9	0.29	60
Perforation 18	4154.0	4155.0	5	14	23.0	0.29	60
Perforation 17	4177.0	4178.0	5	14	22.9	0.29	60
Perforation 16	4199.7	4200.7	5	14	32.2	0.29	60
Perforation 15	4232.0	4233.0	4	14	28.0	0.29	60
Perforation 14	4260.0	4261.0	4	14	20.2	0.29	60
Perforation 13	4280.0	4281.0	4	14	34.5	0.29	60
Perforation 12	4314.6	4315.6	3	14	19.4	0.29	60
Perforation 11	4334.0	4335.0	3	14	24.2	0.29	60
Perforation 10	4358.0	4359.0	3	14	29.9	0.29	60
Perforation 9	4388.0	4389.0	2	14	28.1	0.29	60
Perforation 8	4416.1	4417.1	2	14	26.6	0.29	60
Perforation 7	4442.5	4443.5	2	14	28.9	0.29	60
Perforation 6	4471.7	4472.0	1	6	8.5	0.5	60
Perforation 5	4480.2	4480.5	1	6	8.5	0.5	60
Perforation 4	4488.7	4489.0	1	6	8.5	0.5	60
Perforation 3	4497.2	4497.5	1	6	8.5	0.5	60
Perforation 2	4505.7	4506.0	1	6	8.5	0.5	60
Perforation 1	4514.2	4514.5	1	6	-	0.5	60

Well_3h

Perforation name	Perf top MD (m)	Perf bottom MD (m)	Stage number	No of shots	Perf spacing (m)	Perf diameter (in)	Phasing (deg)
Perforation 48	3346.0	3346.7	15	14	25.0	0.29	60
Perforation 47	3371.0	3371.7	15	14	25.2	0.29	60
Perforation 46	3396.0	3396.7	15	14	29.9	0.29	60
Perforation 45	3426.0	3426.7	14	14	25.0	0.29	60
Perforation 44	3451.0	3451.7	14	14	25.2	0.29	60
Perforation 43	3476.0	3476.7	14	14	29.9	0.29	60
Perforation 42	3506.0	3506.7	13	14	25.0	0.29	60
Perforation 41	3531.0	3531.7	13	14	25.2	0.29	60
Perforation 40	3556.0	3556.7	13	14	29.9	0.29	60
Perforation 39	3586.0	3586.7	12	14	25.0	0.29	60
Perforation 38	3611.0	3611.7	12	14	25.2	0.29	60
Perforation 37	3636.0	3636.7	12	14	29.9	0.29	60
Perforation 36	3666.0	3666.7	11	14	25.0	0.29	60
Perforation 35	3691.0	3691.7	11	14	25.2	0.29	60
Perforation 34	3716.0	3716.7	11	14	29.9	0.29	60
Perforation 33	3746.0	3746.7	10	14	25.0	0.29	60
Perforation 32	3771.0	3771.7	10	14	25.2	0.29	60
Perforation 31	3796.0	3796.7	10	14	29.9	0.29	60
Perforation 30	3826.0	3826.7	9	14	25.0	0.29	60
Perforation 29	3851.0	3851.7	9	14	25.2	0.29	60
Perforation 28	3876.0	3876.7	9	14	29.9	0.29	60
Perforation 27	3906.0	3906.7	8	14	25.0	0.29	60
Perforation 26	3931.0	3931.7	8	14	25.2	0.29	60
Perforation 25	3956.0	3956.7	8	14	29.9	0.29	60
Perforation 24	3986.0	3986.7	7	14	25.0	0.29	60
Perforation 23	4011.0	4011.7	7	14	25.2	0.29	60
Perforation 22	4036.0	4036.7	7	14	29.9	0.29	60
Perforation 21	4066.0	4066.7	6	14	25.0	0.29	60
Perforation 20	4091.0	4091.7	6	14	25.2	0.29	60
Perforation 19	4116.0	4116.7	6	14	29.9	0.29	60
Perforation 18	4146.0	4146.7	5	14	25.0	0.29	60
Perforation 17	4171.0	4171.7	5	14	25.2	0.29	60
Perforation 16	4196.0	4196.7	5	14	29.9	0.29	60
Perforation 15	4226.0	4226.7	4	14	25.0	0.29	60
Perforation 14	4251.0	4251.7	4	14	25.2	0.29	60
Perforation 13	4276.0	4276.7	4	14	29.9	0.29	60
Perforation 12	4306.0	4306.7	3	14	25.0	0.29	60
Perforation 11	4331.0	4331.7	3	14	25.2	0.29	60
Perforation 10	4356.0	4356.7	3	14	29.9	0.29	60
Perforation 9	4386.0	4386.7	2	14	25.0	0.29	60
Perforation 8	4411.0	4411.7	2	14	24.8	0.29	60
Perforation 7	4436.0	4436.7	2	14	30.0	0.29	60
Perforation 6	4466.0	4466.3	1	6	10.0	0.5	60
Perforation 5	4476.0	4476.3	1	6	10.0	0.5	60
Perforation 4	4486.0	4486.3	1	6	10.0	0.5	60
Perforation 3	4496.0	4496.3	1	6	10.0	0.42	60
Perforation 2	4506.0	4506.3	1	6	10.0	0.42	60
Perforation 1	4516.0	4516.3	1	6	-	0.42	60

Table 2: The completion design of the horizontal section of each well

The stages and perforations of each well in relation to the 3D reservoir model and the well trajectories can be visualized in **Figure 3** for a better understanding.

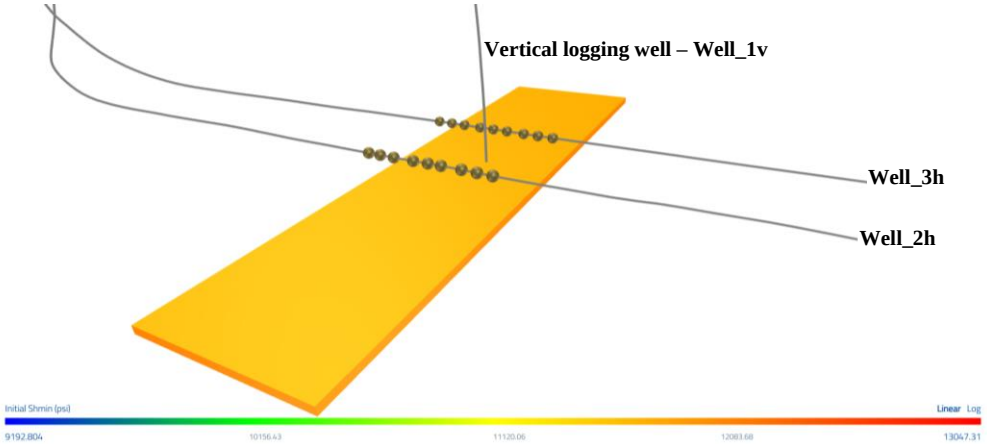

Figure 3: Visualization of the horizontal wells clusters and stages in the 3D reservoir cube

Pumping schedule and stimulation treatment details

The pumping stimulation treatment for stages 6, 7 and 8 of each horizontal well is similar, **Table 3**, with the following characteristics:

Well_2h

Stage Name	Pump Rate bbl/min	Fluid Type	Fluid Volume gal	Prop Conc. ppa	Prop Mass lb	Slurry Volume bbl	Pump Time min	Prop Name
Break Down	3	Slickwater	500	0.00	0	12	4.00	--
Acid	5	15% HCL	2,000	0.00	0	48	9.60	--
Pad	60	Slickwater	30,000	0.00	0	714	11.90	--
0.50 PPA	60	Slickwater	18,000	0.50	9,000	438	7.30	Arena malla 100
1.00 PPA	60	Slickwater	18,000	1.00	18,000	448	7.47	Arena malla 100
1.50 PPA	60	Gel Lineal #25	20,000	1.50	30,000	509	8.48	Arena malla 100
2.00 PPA	60	Gel Crosslink #25	20,000	2.00	40,000	519	8.65	Arena malla 100
0.50 PPA	60	Gel Crosslink #25	24,000	0.50	12,000	582	9.70	Wanli 30/50
1.00 PPA	60	Gel Crosslink #25	18,000	1.00	18,000	444	7.40	Wanli 30/50
1.50 PPA	60	Gel Crosslink #25	18,000	1.50	27,000	452	7.53	Wanli 30/50
2.00 PPA	60	Gel Crosslink #25	18,000	2.00	36,000	460	7.67	Wanli 30/50
2.30 PPA	60	Gel Crosslink #25	20,000	2.30	46,000	516	8.60	Wanli 30/50
2.60 PPA	60	Gel Crosslink #25	20,000	2.60	52,000	522	8.70	Wanli 30/50
3.00 PPA	60	Gel Crosslink #25	18,000	3.00	54,000	476	7.93	Wanli 30/50
3.50 PPA	60	Gel Crosslink #25	16,000	3.50	56,000	430	7.17	Wanli 30/50
4.00 PPA	60	Gel Crosslink #25	16,000	4.00	64,000	437	7.28	Wanli 30/50
4.50 PPA	60	Gel Crosslink #25	16,000	4.50	72,000	444	7.40	Wanli 30/50
Flush	60	Slickwater	10,137	0.00	0	241	4.02	--
			302,637		**534,000**	**7,680**	**136.80**	
			1145	m^3				

Well_3h

Stage Name	Pump Rate bbl/min	Fluid Type	Fluid Volume gal	Prop Conc. ppa	Prop Mass lb	Slurry Volume bbl	Pump Time min	Prop Name
Break Down	3	Slickwater	500	0.00	0	12	4.00	--
Acid	5	15% HCL	2,000	0.00	0	48	9.60	--
Pad	60	Gel Crosslink #25	20,000	0.00	0	476	7.93	--
0.50 PPA	60	Gel Crosslink #25	10,000	0.50	5000	243	4.05	Arena malla 100
1.00 PPA	60	Gel Crosslink #25	20,000	1.00	20000	498	8.30	Arena malla 100
1.00 PPA	60	Gel Crosslink #25	5,000	1.00	5000	123	2.05	Unimin 30/50
2.00 PPA	60	Gel Crosslink #25	15,000	2.00	30000	383	6.38	Unimin 30/50
3.00 PPA	60	Gel Crosslink #25	15,000	3.00	45000	397	6.62	Unimin 30/50
3.50 PPA	60	Gel Crosslink #25	20,000	3.50	70000	537	8.95	Unimin 30/50
4.00 PPA	60	Gel Crosslink #25	20,000	4.00	80000	546	9.10	Unimin 30/50
4.50 PPA	60	Gel Crosslink #25	10,000	4.50	45000	277	4.62	Unimin 30/50
5.00 PPA	60	Gel Crosslink #25	7,000	5.00	35000	197	3.28	Unimin 30/50
5.00 PPA	60	Gel Crosslink #25	7,000	5.00	35000	197	3.28	Wanli 30/50
5.50 PPA	60	Gel Crosslink #25	10,000	5.50	55000	286	4.77	Wanli 30/50
6.00 PPA	60	Gel Crosslink #25	10,000	6.00	60000	291	4.85	Wanli 30/50
6.50 PPA	60	Gel Crosslink #25	10,000	6.50	65000	295	4.92	Wanli 30/50
Flush	60	Slickwater	10,133	0.00	0	241	4.02	--
			191,633		**550,000**	**5,035**	**92.72**	
			725	m^3				

Table 3: Pumping schedule and stimulation treatment details

Production history and fluid PVT data

Using the PVT data provided and utilizing the software standard Black Oil Model PVT correlations, we generated the PVT variable curves obtained as a function of pressure (**Figure 4**). The same PVT model was used for both horizontal wells, even though each well landed on different shales. Actual data confirm that the fluids produced from both formations have similar PVT properties, confirming this assumption.

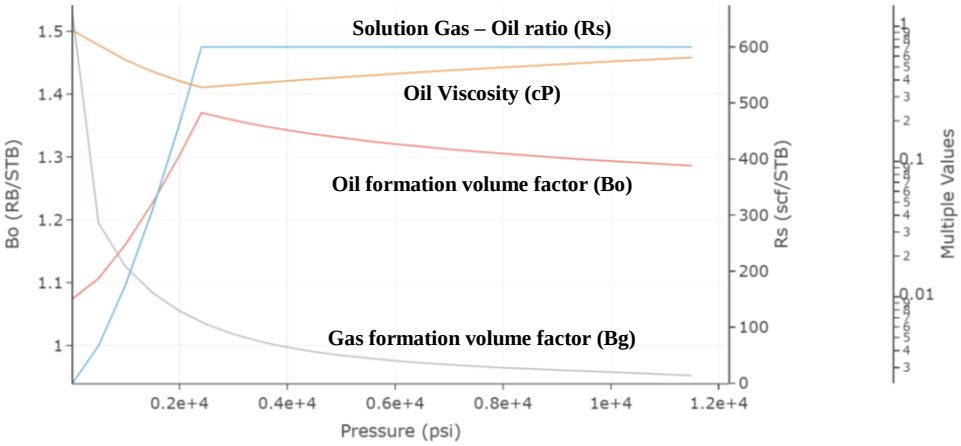

Figure 4: Software standard black oil model PVT correlations curves

Figure 5 shows three (3) years production history for each well, with the fifteen (15) stages flow rates of each fluid phase linearly prorated to three (3) stages per well.

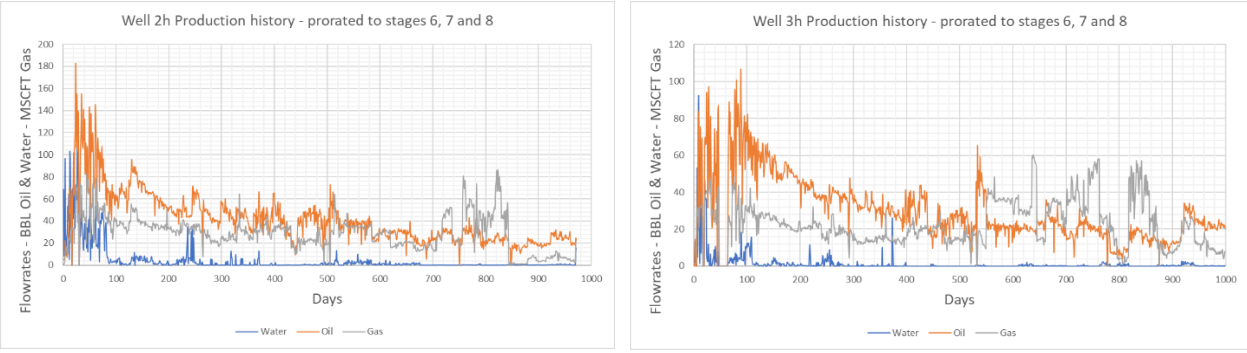

Figure 5: Production history linearly prorated to three (3) stages per well

Microseismic data

According to the microseismic data in **Table 4,** the average fracture size is as follows:

	AVERAGE FRAC SIZE			
Microseismic	**Length wing - wing (m)**	**Length wing - wing (ft)**	**Heigth (m)**	**Heigth (ft)**
Well 3h	267	878	98	321
Well 2h	480	1578	160	527

Table 4: Average frac size as per the microseismic data

Analysis focus and scenarios

To investigate the parent-child well phenomenon in this project, fictitious child wells are drilled and stimulated in the vicinity of an existing well, the parent well. The objective is to measure the impact of the parent-child effect on the child well EUR under several cases, considering two key variables, well spacing and parent well depletion, and three scenario groups.

***Single child well vs. parent well*:** the impact of the parent-child effect is evaluated in term of the EUR of a single child well located at different distances from the parent well and the parent depletion time intervals as detailed below. Two sets of sensitivities are run, one for the lower interval of T4 unit and the other for the T2 unit.

- Well spacing 200m, parent well depletion time: 1, 2, 3, 4 and 5 years
- Well spacing 300m, parent well depletion time: 1, 2, 3, 4 and 5 years
- Well spacing 400m, parent well depletion time: 1, 2, 3, 4 and 5 years
- Well spacing 600m, parent well depletion time: 1, 2, 3, 4 and 5 years

Twenty (20) sensitivities are run for each interval, for the total of forty (40).

Two simultaneous child wells vs two single child wells: two child wells are drilled and stimulated simultaneously, located at 300m and 600m respectively from the parent well. Their EUR performance is compared to the performance of their respective 300m single child well and 600m single child well. The same parent well depletion time intervals are used.

- *Well spacing sensitivities:* Two simultaneous child wells, 300m and 600m, vs. the 300m single child well and the 600m single child well. One (1) sensitivity per interval.
- *Parent well depletion time sensitivities*: 1, 2, 3, 4 and 5 years. Five (5) per interval.

As in the previous case, two sets of sensitivities are performed, one for the lower interval of T4 unit and the other for the T2 unit. A total of ten (10) sensitivities are run, five (5) per interval.

***Improved completion design child well vs the original completion design child well*:** the EUR performance of a single child well of the original completion design and located at 300m from the parent well is compared to the same single child well with an improved completion design.

- *Original completion design*: three (3) clusters per stage, with a stimulation fluid volume per cluster of 380m3 for the lower interval of T4 unit and 240m3 for the T2 unit.
- *Improved completion design*: nine (9) clusters per stage, with a stimulating fluid volume per cluster of 127m3 for the lower interval T4 unit and 80m3 for the T2 unit.

The sensitivities for each interval are five (5) for a total of ten (10), below the details:

- *Well spacing sensitivities:* original completion design 300m single child well vs the improved completion design 300m single child well. One (1) sensitivity per interval
- *Parent well depletion time sensitivities*: 1, 2, 3, 4 and 5 years. Five (5) per interval

The remaining variables, including but not limited to, are held constant or equal between each parent and child well:

- *Unconventional stimulation techniques:* proppant types and quantities, fluid types and volumes, pumping schedules, etc.
- *Completion design (except in the 3rd group):* number of stages, clusters per stage, number of perforations, orifice angle and diameter per cluster, casing type and size, survey, etc.
- *Static petrophysical and geomechanical model:* porosity, permeability, Shmin, SHmax, Sv, water saturation, pore pressure, Young´s modulus, etc.

The impact on the child well EUR in each sensitivity analysis is calculated using **Equation 1**:

$$\Delta\, \boldsymbol{EUR\ in}\ \% = \frac{\boldsymbol{Child\ well\ EUR\ 20y - Stand\ alone\ well\ EUR\ 20y}}{\boldsymbol{Stand\ alone\ well\ EUR\ 20y}}$$

Equation 1: Delta EUR in %

- *Δ EUR in %:* delta of EUR generated in the child well due to the parent-child effects.
- *Child well EUR 20y period:* the EUR of the child well in the BOE after 20 years of production since it was drilled and stimulated.
- *Stand-alone well EUR 20y period:* the EUR of the stand alone or correspondent parent well in BOE after 20 years of production since it was drilled and stimulated

Project development

While collecting and processing all the necessary data is critical, calibrating the simulations is just as important as this initial step. Prior to simulating the sensitivities mentioned above, considerable time and effort was spent in the calibration process, to ensure that the results would be representative of the real well observed data. The calibration process was divided into three main steps: calibration of fracture geometry and physics, calibration of the flow rates using real production history as a reference and calibration of the long term cumulative production and EUR over time.

Calibrating the fracture geometry and physics

In **Figure 6**, the initial fracture geometry and physics simulation using the default software settings and the original logging data from the 3D static reservoir model produced these results:

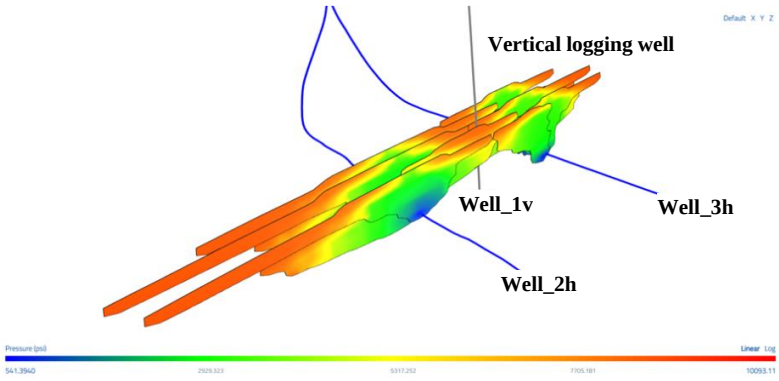

Figure 6: Initial fracture model and geometry results using the standard setting and initial data

The general observations in this first output are as follows: excessive fracture length or wing to wing fracture dimensions in both wells, which also communicate with each other. Excessive fracture growth height in both cases, especially upward. Well_3h barely stimulated its pay zone, the T2 unit, with its fractures mostly stimulating the Well_2h shale, the lower interval of T4 unit.

This fracture geometry didn´t resemble the geometry data provided by the microseismic and previously calibrated old simulations made by the production engineers. The fracture geometry and physics results should be consistent with the confirmed field observations:

- Fracture height growth from Well_3h should not reach the lower interval of T4 unit.
- The fracture height from Well_2h is confined to the lower interval of T4 unit.
- There is no communication between the two wells.
- Average fracture length and height should match the microseismic data (Table 4).

Adjustments were made to simulate the barrier effect between the two landing zones, preventing fractures from growing upward and communicating between the two wells, using a two-step approach:

1. Adjustment of Shmin and permeability in the 3D static model to provide the required barrier effect.
2. Adjust the following fracture settings and parameters: isotropic pressure dependent permeability factor (leak-off), tortuosity and fracture toughness.

These modifications were applied to the Shmin, permeability and the 3D static reservoir model:

- The reduction of the layer thickness in the 3D model, from 10m to 1m, in order to better detect Shmin variations, e.g. barriers, mainly peaks.
- The initial permeability values obtained were too high. A multiplier factor of 0.007 was applied, resulting in values typical of unconventional shales.
- By running simulations and observing the fracture height growth results, and adjusting the Shmin values in each model, the desired barrier effect between zones was achieved, with an overall 5% increase in Shmin values throughout the reservoir model, except for the Shmin peaks acting as barriers, which were increased by 20% of their original value.

Figure 7 shows the resulting permeability and Shmin variables plotted against depth.

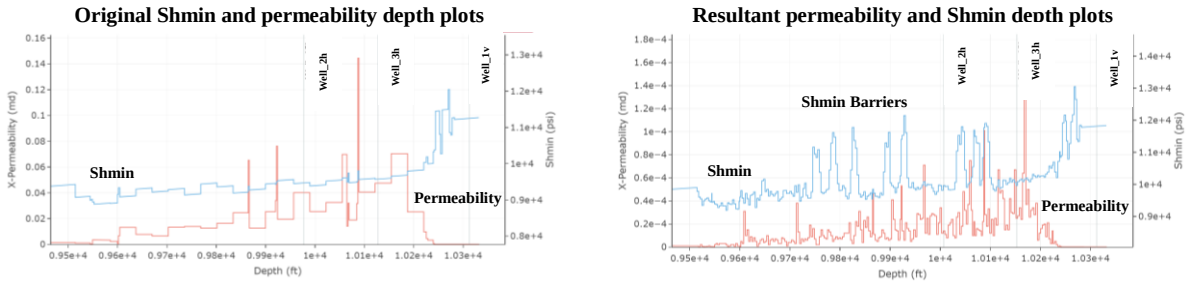

Figure 7: Permeability and Shmin plots as a function of depth

While these changes successfully simulated the presence of the barrier, the fracture geometry and physical properties did not yet reflect similar characteristics to the actual fractures. Also, the ISIP values observed during the real stimulation treatment differed from those obtained from the simulations. The isotropic permeability factor (leak-off), tortuosity and fracture toughness settings were modified to further calibrate the fracture geometry and physics. Details in **Table 5**

Setting name	Default value	Adjusted value
Isotropic Permeability Factor (Leak-Off)	None	Check below
Tortuosity	Exponent and coefficient: 0 & 0	Exponent and coefficient: 0.5 & 20
Fracture Toughness	0	0.05
Isotropic Permeability Factor (Leak-Off)		
Delta Pressure (PSI)	**Permeability multiplier along Shmin**	
1094	1080	
514	180	
0	1	

Table 5: Isotropic permeability factor (leak-off), tortuosity and fracture toughness settings

In **Figure 8,** the calibrated fracture model, replicates the geometry and physics observed in the microseismic data and the WHP pressures (ISIP)

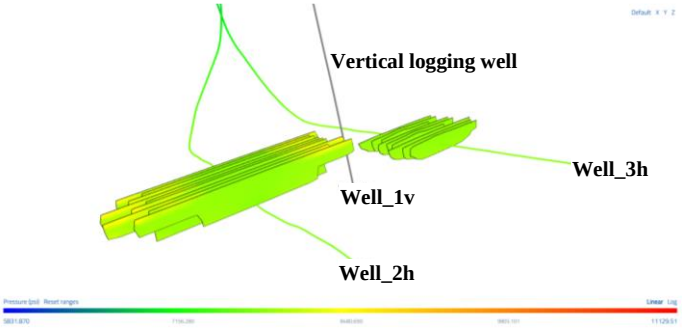

Figure 8: Calibrated fracture model

Flow rates calibration using real production history

An initial run was performed using the original PVT properties, relative permeability data and production history to evaluate the cumulative production results and simulated production history. The **dashed curves represent the actual data and the solid curves represent the simulation results.**

Figure 9 shows the results with comments for Well_2h, lower interval of T4 unit, prior calibration:

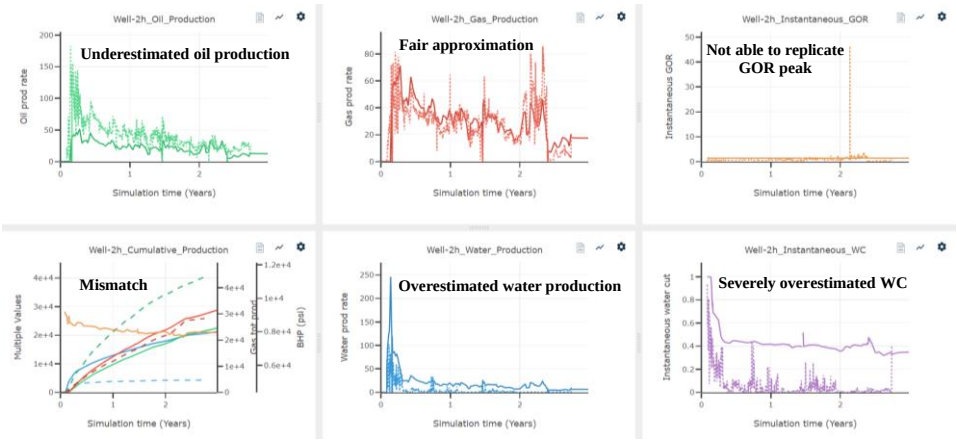

Figure 9: Well_2h initial simulated flowrates and cumulative production vs real production data

Figure 10 shows the results with comments for Well_3h, T2 unit, prior calibration:

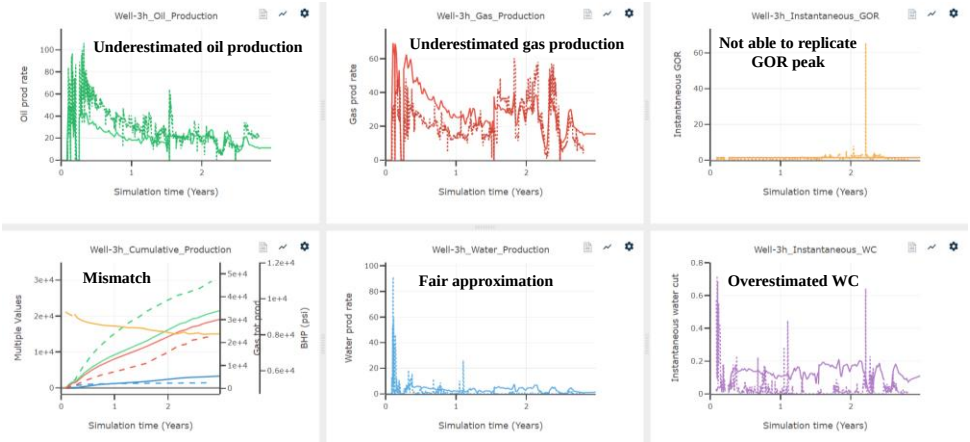

Figure 10: Well_3h initial simulated flowrates and cumulative production vs real production data

The initial simulated production from both wells shows discrepancies with the real production data (above or below the measured values), it was decided to proceed as follows:

1. Divide the 3D static model into two sections, the lower interval of T4 and T2 unit, and apply separate permeability multipliers.
2. In the Brooks-Corey model, **Equation 2**, adjust the relative permeability parameters for each flow phase in each interval.

$$Krp = Krpm * \left(\frac{Sp - Srp}{1 - Srp}\right)^{np}$$

Equation 2: Brooks-Corey relative permeability model equation

- Krp = phase relative permeability
- Krpm = phase relative permeability multiplier
- Sp = phase saturation
- Srp = residual phase saturation
- Np = Brooks-Corey phase exponent

The permeability multipliers and relative permeability parameters used for the final calibration are shown in **Figure 11** and **Table 6**:

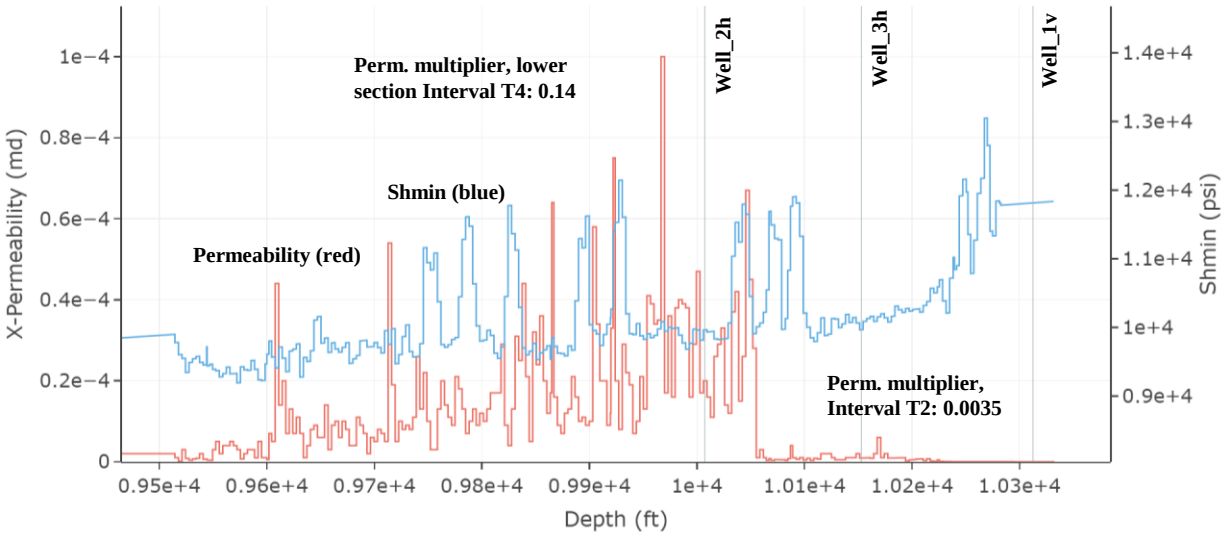

Figure 11: Permeability adjusted by multipliers as function of shales depth

Brooks Corey permeability parameters Well_2h	Water Phase	Oil Phase	Gas Phase
Max. Residual Saturation (Srp)	0.4	0.2	0.001
Brooks-Corey Phase Exponent (np)	3	2	1
Relative perm. Multiplier (Krpm)	0.1	1	1
Brooks Corey permeability parameters Well_3h	**Water Phase**	**Oil Phase**	**Gas Phase**
Max. Residual Saturation (Srp)	0.4	0.2	0.001
Brooks-Corey Phase Exponent (np)	3	2	1
Relative perm. Multiplier (Krpm)	0.5	1	2

Table 6: Adjusted settings of the Brooks-Corey relative permeability model

Applying the above multipliers to the total permeability affected the previously calibrated fracture physics and geometry. The permeability reduction resulted in excessive fracture growth, forcing the leakage, fracture toughness, and conductivity settings to be revised to recalibrate the fracture model without affecting the production history match. The isotropic permeability factor (leak-off) was again individually adjusted for each of the wells. The fracture toughness and the aperture conductivity factors were adjusted equally for both wells. Details in **Table 7.**

Setting name	Default value	Adjusted value
Isotropic Permeability Factor (Leak-Off)	Details in **Table 5**	Check below
Tortuosity	0.4	0.25
Fracture Toughness	0.05	0.25
Isotropic Permeability Factor (Leak-Off) - After production calibration Well_2h		
Delta Pressure (PSI)	**Permeability multiplier along Shmin**	
1212	467	
632	1	
0	1	
Isotropic Permeability Factor (Leak-Off) - After production calibration Well_3h		
Delta Pressure (PSI)	**Permeability multiplier along Shmin**	
1279	609	
698	1	
0	1	

Table 7: Further fracture modelling settings adjustment after simulated production calibration

The recalibrated fracture model (**Figure 12**) resulted in a fracture geometry with less symmetry and more irregular shape compared to the original fracture calibration, but still within the range of microseismic observations.

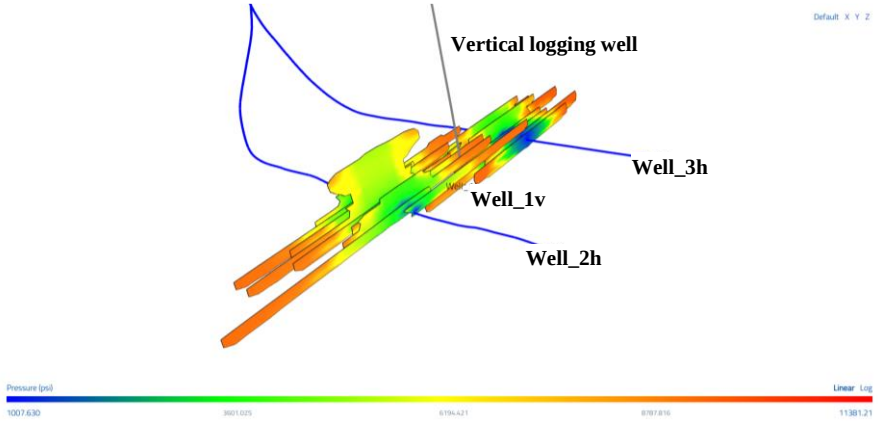

Figure 12: Recalibrated fracture model and geometry after simulated production calibration

An almost perfect simulated production match was achieved for the Well_2h as shown in **Figure 13**. All the three simulated phases follow the real data plot trends, with averages that match the actual production history measurements. Most importantly, the cumulative production trends replicate the real well behavior, providing confidence that the model will be able to accurately reproduce the expected EUR over a period of 20 years.

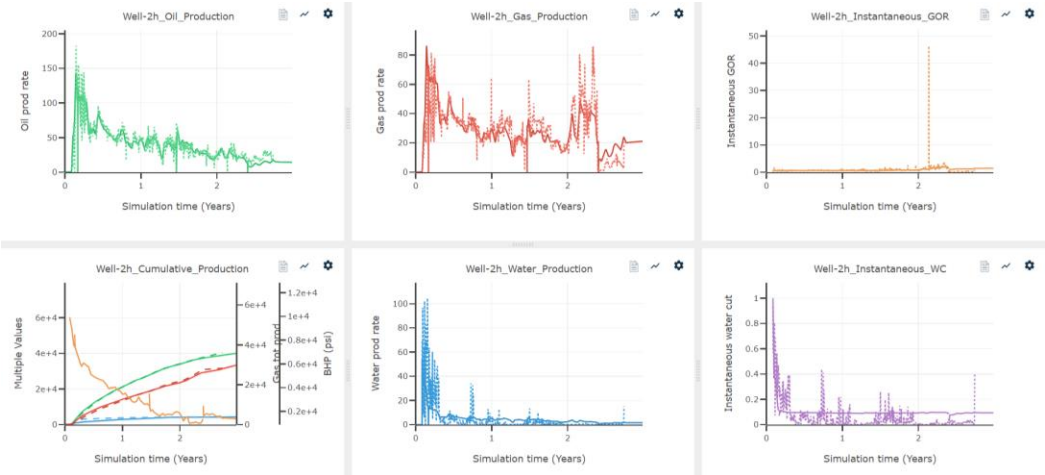

Figure 13: Well_2h calibrated flowrates and cumulative production vs real production data

For Well_3h (**Figure 14**) the production adjustment results were not identical as in the previous case but were close to the overall well performance at the time. Differences between the simulations and the actual data are observed in the oil and gas phase flow rates after 18 months of well operation. The difference is more significant in the gas phase, of greater magnitude and over a longer period of time. In both cases, after a period of 30 months, the modeled flow rates have an improved match to the magnitudes and patterns of the dotted lines (the field flow rate measurements). The main objective is to be able to reproduce the cumulative production patterns that form the basis of the EUR estimates on a long-term basis rather than short-term production trends.

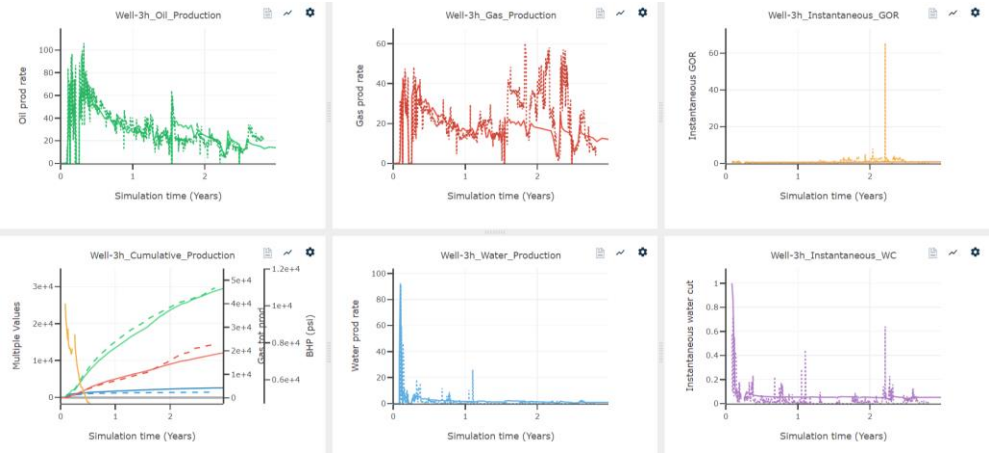

Figure 14: Well_3h calibrated flowrates and cumulative production vs real production data

The PVT variables were held constant and no adjustments were made during this calibration process. A threshold of 1000psi of flowing BHT at the average TVD of the horizontal sections of the two wells was set to ensure that the software did not overestimate production at the expense of unrealistically low BHP values.

Calibration of the long-term cumulative production and EUR over time

At this point, the intent is to reflect EUR curves with a flattening tendency after a 20 year of production, based on experiences with similar wells in the area. The default settings gave us the following 20y EUR curves for Well_2h and Well_3h (**Figure 15**):

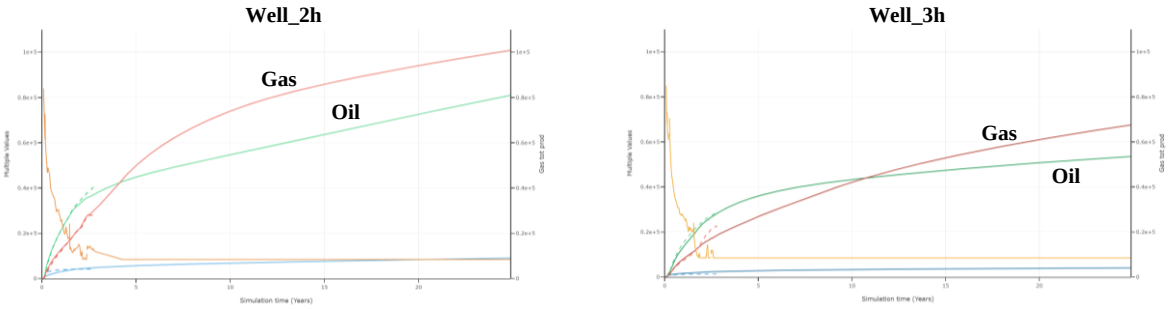

Figure 15: Cumulative production over a 20y time period with default settings (no proppant conductivity loss)

These types of wells reach a severe fracture conductivity loss somewhere after 20 years of production, when the cumulative curves are almost flat. The software settings, by default, doesn´t take fracture conductivity loss beyond the user supplied proppant conductivity curves into account, so both wells will continue to have a steadily cumulative increase after this time of 20 years, which is not considered a common behavior.

Considering that in most unconventional wells proppant degradation and embedding occurs during the life of the well. A proppant degradation coefficient of 0.0002 was considered for both wells, the default being

0, for all the proppant types used. This coefficient is a multiplier with a unit of 1/day that linearly affects the proppant conductivity correlations, hence rates. The larger the number, the greater the effect. The resulting EUR curves are shown in **Figure 16**, and reflect the well performance loss tendency of these types of wells.

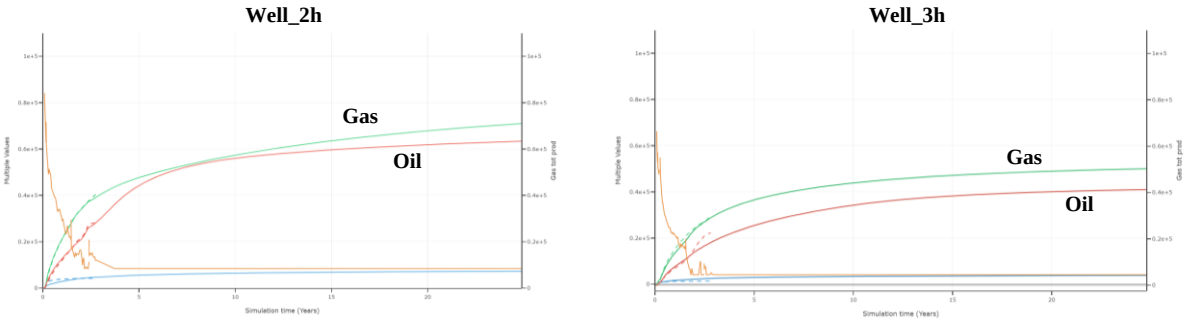

Figure 16: Calibrated cumulative production over a 20y time period considering a proppant conductivity loss factor

Project results and conclusions

The results of this project are presented according to the three main scenarios previously mentioned for each landing zone.

Single child well spacing – Lower Interval of T4 unit

In **Figure 17**, the 200m and 300m cases show a sudden increase in the parent-child effect after one year, indicating that with a moderate depletion of the parent well, the impact can be severe, especially in proximity (200m case). After year 1, the parent-child effect increases at a slower rate as the parent well depletion interval increases, for simplicity and practical purposes, the relationship can be approximated by linear curves for both cases. While obvious, the negative impact on the EUR in the 300m curve is significantly reduced in all depletion cases, on average 17% less than in the 200m curve.

The 400m curve shows that the EUR of the child well is less affected by the depletion time interval of the parent well, with the effect remaining almost constant after the year 1, with only a slight decrease in EUR. The increase in the parent-child effect at larger depletion time intervals no longer holds at significant well spacing, 400m and beyond, and remains constant regardless of depletion.

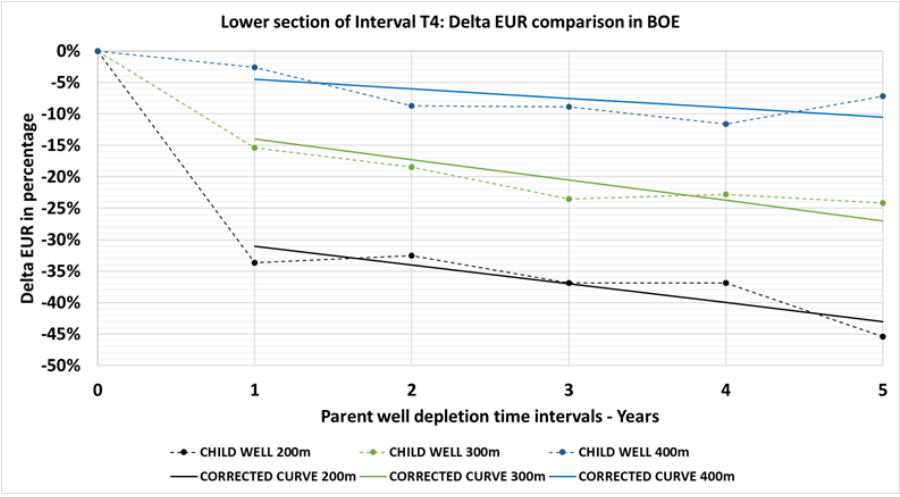

Figure 17: Delta EUR curves, Single child well spacing – lower interval of T4 unit

In the case of 600m well spacing, the child well delta EUR curves ranges from 0 to 9% over all the depletion intervals. The interpretation is that at 600m spacing, the parent-child effect no longer affects the child well, and has no impact on its EUR. Therefore, the curves for 600m well spacing have been removed from **Figure 17**. **Figure 18** shows that the parent well and the child wells have depleted different stimulated reservoir volumes, with almost no interaction with each other. The EUR performances of both wells are similar.

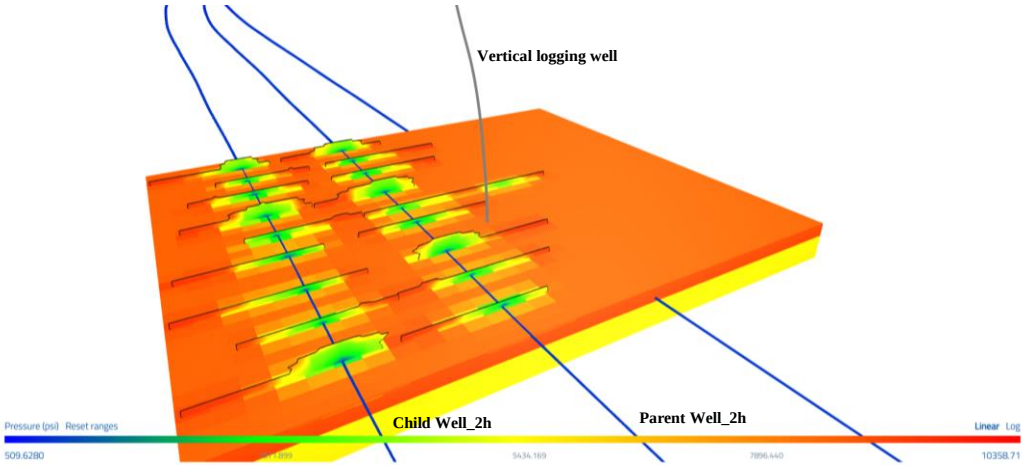

Figure 18: Fracture model image, lower interval of T4 unit - single child well 600m spacing after 25 years of depletion

Single child well spacing – T2 unit

In **Figure 19**, the relationship between well spacing and the parent-child effect is clear, as in the previous case, the closer the spacing, the greater the effect. In the case of 200m well spacing, this effect is on average twice as large as in the other two cases, 300m and 400m well spacing.

The positive and negative EUR performances of the 600m spacing child well are due to the margin of error of the simulations and can be considered as zero for practical purposes, there is no parent-child effect impact. As in the previous scenario of the lower interval T4 unit, the 600m delta EUR case is removed.

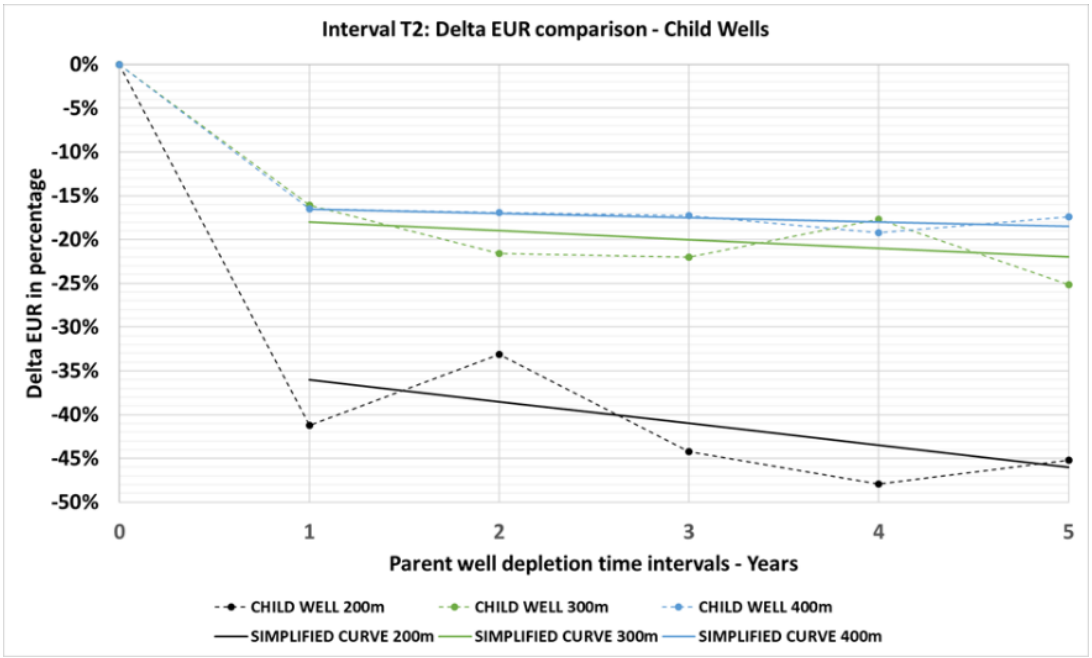

Figure 19: Corrected delta EUR curves, Single child well spacing – T2 unit

In **Figure 20**, in the case of 600m well spacing, it is observed that the two stimulated reservoir volumes are separated.

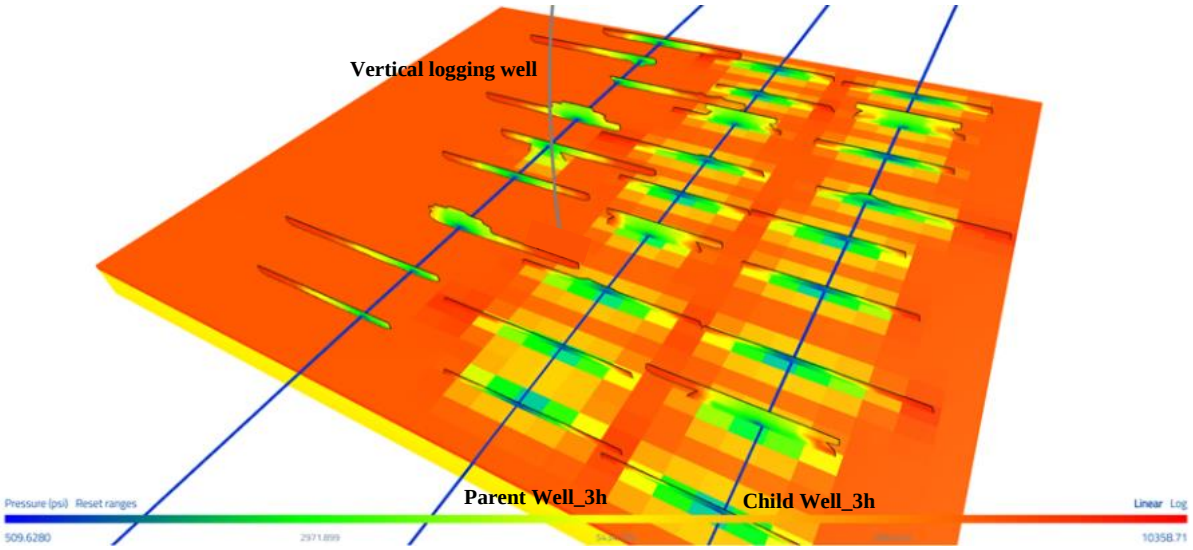

Figure 20: Fracture model image, T2 unit single child well with 600m spacing after 25 years of depletion

In summary, the parent-child effect increases as the child well spacing decreases and the parent depletion increases:

- This is clearly observed in the case of 200m spacing curve, although the variability of the delta EUR results is most notorious in year 1 and year 2. This is easier to see when looking at all the intervals together and by adding a linear trend curve. It is important to remember that there are other causes besides the parent-well effect that can have an impact on the wells EUR performance, as this is the source of the variability of the delta EUR points. It is worth noting that a moderate depletion of the parent well (year 1) already has a significant negative effect on the child EUR.
- The case of 300m spacing shows a similar behavior, but with less variability after year 1 and a potentially slight tendency for EUR to decrease over larger depletion intervals if a linear trend curve is added. However, a flat linear tendency curve would also fit, assuming a constant average delta EUR over the depletion intervals.
- In the case of 400m well spacing, the delta EUR value is stable after year 1. There is no interaction between the depletion of the parent well and the parent-child phenomenon. An interesting observation is that the 300m delta EUR curve and this one have similar values and trend. That is, in the case of the lower interval of T4 unit, the average delta EUR value is -21% at 300m and -9% at 400m. In the T2 unit, these values are -20% and -17.5% respectively.

Two simultaneous child wells – Lower Interval of T4 unit

The objective is to understand whether or not the parent-child interactions are magnified by the simultaneous stimulation of two child wells and to quantify the impact on their EUR. In **Figure 21**, when comparing the delta EUR curve from the 300m simultaneous child well to the 300m single child well, the EUR performance worsens by an additional -5% on average between the two curves, confirming that the magnitude of the parent-child interaction is greater across all the parent well depletion intervals. This is valid when the outlier point is removed from the linear trend calculations.

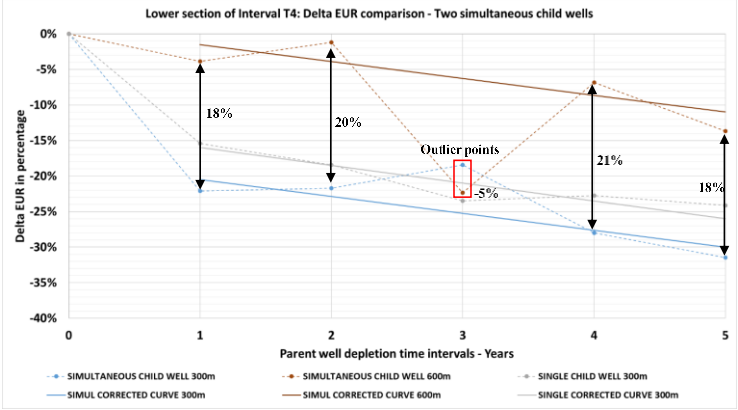

Figure 21: Corrected delta EUR curves, two simultaneous wells – Lower interval of T4 unit

Regarding the case of 600m simultaneous child well (**Figure 21),** there is confirmation that this well is affected by the parent-child effect, which is stronger at longer depletion intervals. Although the impact on the EUR performance is moderate, ranging from -4% to -14% depending on the time interval, it is present and must be accounted for, unlike the 600m single child well case (removed from the plots) which is no longer affected by the phenomenon under this set of conditions and well design. Overall, both simultaneous child wells suffer from an increased impact of the parent-child effect when compared to their single well counterparts.

When analyzing the difference between the EUR deltas from the cases of 600m and 300m simultaneous child wells, in years 1, 2, 4 and 5, the values remain almost constant, ranging from 18% to 21% within the expected margin of error. In the point of year 3, the outlier point, this value jumps to -5% in favor of the 300m simultaneous child well EUR performance. In the year 3 sensitivity results (**Figure 22**), the outer 600m simultaneous child well presents damage in some clusters, hence the abnormal EUR performance. As per this sensitivity, cluster damage is the result of undesired interactions of both wells stimulating volumes during the zipper frac stimulation treatment, something not related to the parent-child effect.

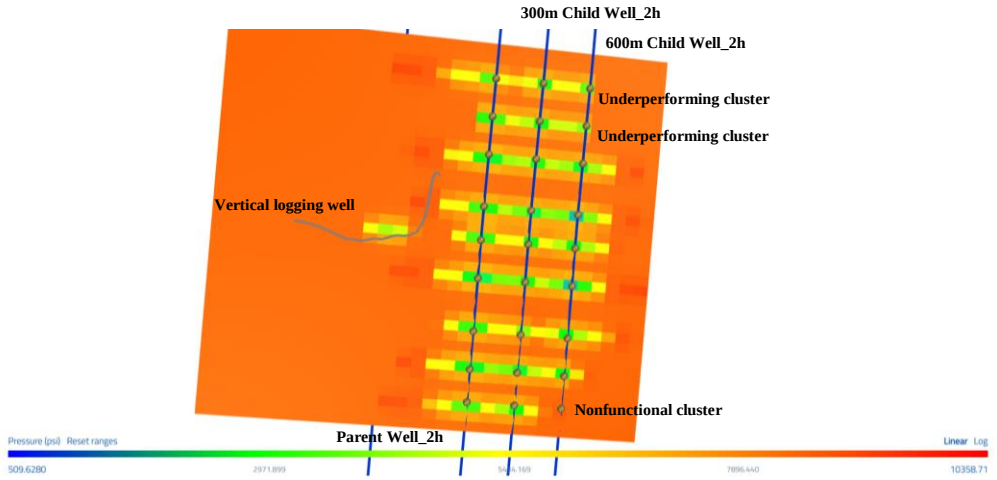

Figure 22: Drainage area of the two simultaneous child wells, lower interval of T4 unit – parent well depletion year 3

Two simultaneous child wells –T2 unit

In **Figure 23**, starting with the 300m delta EUR curves, this simultaneous child well has an additional EUR drop of 8% on average when compared to the single child well. As in the lower interval of T4 unit, there is an increase in the parent-child interaction when two child wells are simultaneously stimulated with this completion design, spacing and reservoir static conditions.

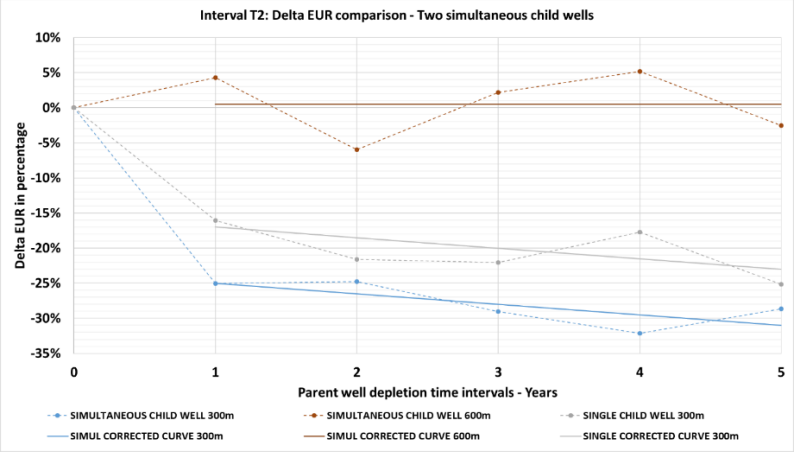

Figure 23: Corrected delta EUR curves, two simultaneous wells – T2 unit

Although slight, there is a tendency for the parent-child interaction to increase at longer depletion time intervals for these the two wells. The 300m simultaneous child well curve shows more stable delta EUR values than its counterpart in the lower interval of T4 unit, indicating that other negative interactions such as screen outs, cluster inefficiencies, etc. are more attenuated and thus less likely to occur.

The 600m simultaneous child well is not affected by the parent-child phenomenon. While its curve shows positive and negative delta EUR values, when averaged, the resulting flat linear curve average values is 0.5%, interpreted as non-interaction between the parent depletion zone and the child well. The variability at the delta EUR points in this curve is due to other causes other than the parent-child effect. The case of the 600m single child well is not shown because, as in the previous cases, it is not affected by the phenomenon.

Cluster density increase per stage – Lower Interval T4 unit

Figure 24 shows that the child well with a higher number of clusters has a more continuous effective drainage area (blue, green, yellow and light orange) compared to the parent well with the original completion design, even though some of the clusters do not show drainage. An important observation is that the difference in drainage between the two wells confirms that there is less interaction between the two wells, so that two separate volumes of stimulated reservoir are being produced, rather than a single volume being produced by two wells.

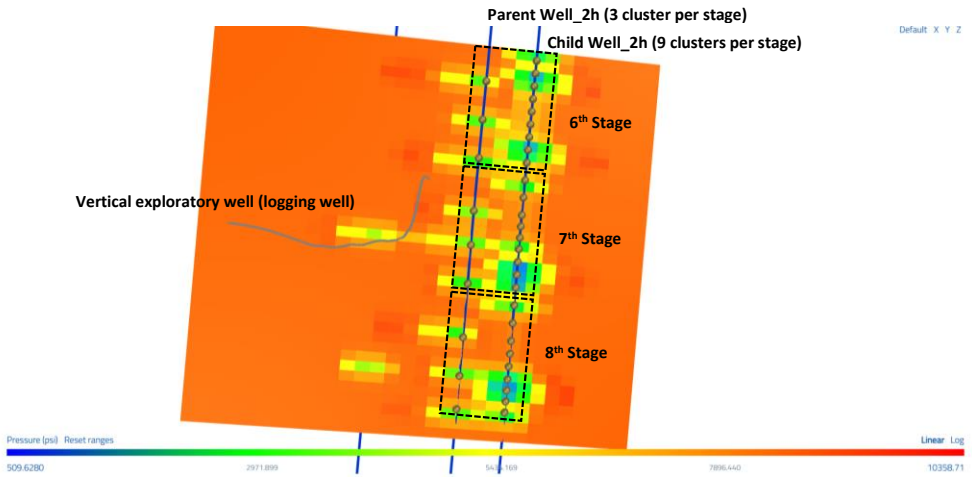

Figure 24: Drainage volume, 300m high cluster density child well and parent well, lower interval of T4 unit

Figure 25 shows a positive EUR performance of the child well with high cluster density from years 0 to 3 when compared to the parent well despite the parent-child interaction. This is expected since the goal of the improved completion design is to increase the EUR of the well. The parent-child effect is present, but it is offset during the first three years and considerable attenuated in the last two years. Both wells are affected by the parent-child phenomenon. After adding the lineal trend curves, not only is it confirmed that the parent-child effect increases in both wells as the depletion time increase, but also the impact of this interaction can be considered equal in practice for both wells, but with an average 25% of EUR improvement in the child well with higher cluster density.

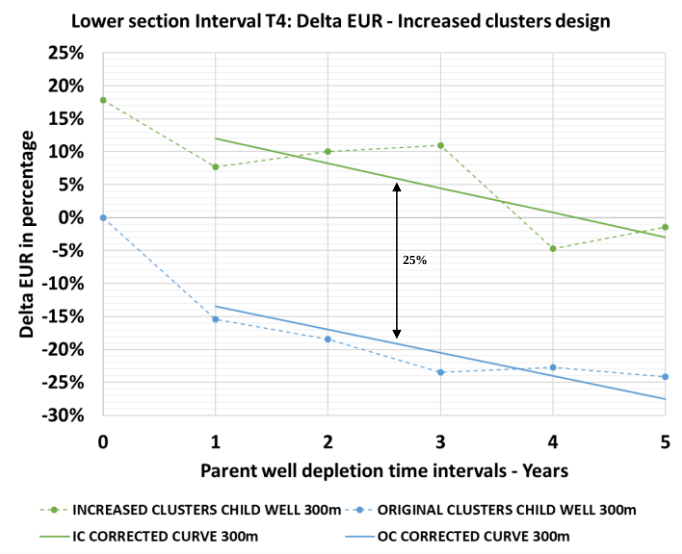

Figure 25: Corrected delta EUR curves, cluster density increase per stage – lower interval of T4 unit

Cluster density increase per stage –T2 unit

In **Figure 26**, the top view of the drainage volume of the higher density cluster child well versus its parent well with the original completion design shows the difference between their drainage efficiencies. The drainage area of the child well is almost continuous along the horizontal section, with most of the clusters producing effective drainage, indicating low pressures around them (blue and green colors). The opposite is true for the parent well, with less effective drainage around the clusters and higher pressures, which is also a non-continuous volume over the horizontal section.

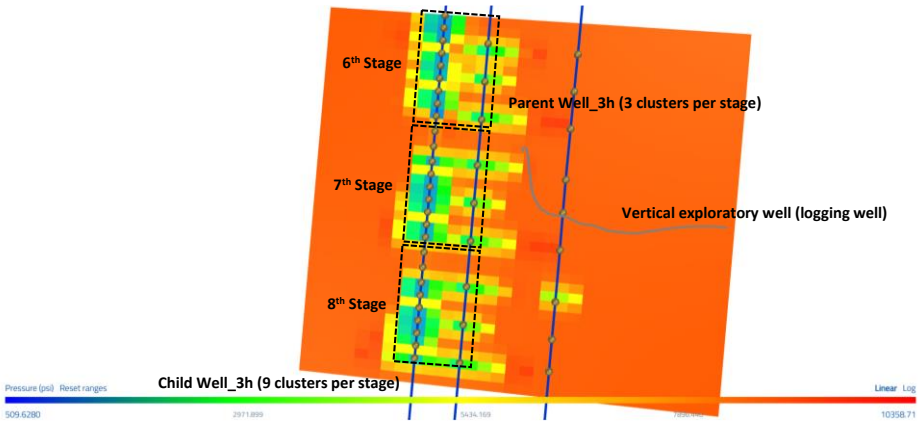

Figure 26: Drainage volume, 300m high cluster density child well and parent well, T2 unit

Linear projection of the curves in **Figure 27** confirms that both wells are affected by the parent child effect. However, the higher density cluster child well has a positive delta EUR performance over all the depletion

intervals. On average, the delta EUR performance difference between these wells is 51% in favor of the improved completion design child well. An improved completion design will significantly reduce or even eliminate the parent-child effects as seen in both shales, the lower interval of T4 unit and the T2 unit.

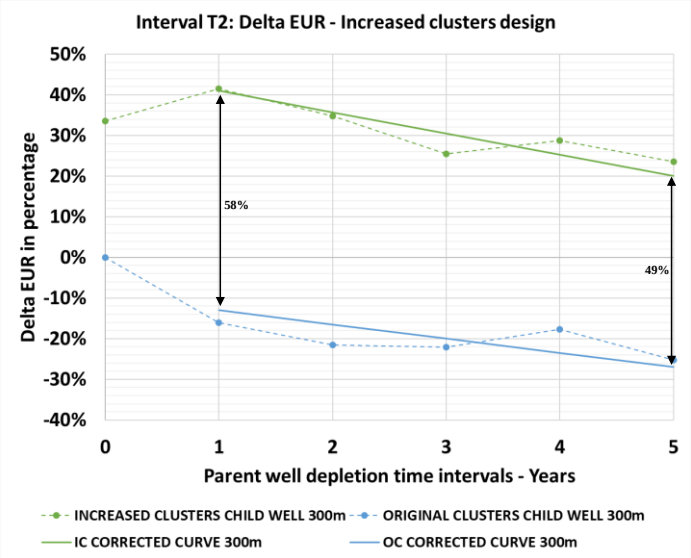

Figure 27: Corrected delta EUR curves, cluster density increase per stage –T2 unit

Summary and conclusions

The parent-child effect across the different scenarios in the EUR child well can be summarized as follows, always considering this is only valid for the hub core of Vaca Muerta:

- Corroborate that well spacing between parent and child wells is one of the main drivers of the parent-child phenomenon; as the well spacing decreases, the parent-child effect increases.
- For this conceptual model (hub core of Vaca Muerta) and fracture designs, the parent-child effect effectively disappears when the spacing between the parent and child well is greater than 600m.
- The level of depletion of the parent well has a relevant impact on the parent-child effect, with greater depletion tending to increase the effect, especially in the early years, but is not a major driver compared to well spacing.
- At closer well spacing (200m and 300m), the greater the depletion of the parent well the greater the parent-child effect, in a trend that approximates a linear curve.
- At 400m well spacing, after parent well depletion intervals of 1 or 2 years, the parent-child phenomenon remains constant and is no longer affected by the level of depletion.
- The parent-child interaction in two simultaneous child wells, located at 300m and 600m respectively, is greater than that of their single child well counterparts. In the 600m spacing simultaneous child well, the parent-child effect is observed in the lower interval of T4 unit.
- The relationship between well spacing and parent well depletion (parent-child effect) for the two simultaneous child wells cases remains the same, with well spacing being the main driver.
- A child well with an improved completion design can significantly or completely offset the parent-child interaction by having a better EUR performance than the parent well, depending on the case. The parent-child effect is present, but its negative effect can be compensated by a better completion design.

- For the case of the new completion design child well at 300m spacing, the greater the depletion of the parent well the greater the impact of the parent-child effect. While the delta EUR performance can be positive over all the depletion time intervals, this better performance is reduced as depletion increases, following an approximated linear trend.

Acknowledge

The authors would like to thank YPF S.A. for the provision of the datasets used during the project and ResFrac for the license provision for the use of their academic version software.

References

Ratcliff Dave, Mark McClure, Garrett Fowler, Brendan Elliot and Austin Qualls., 2022. "Modelling of Parent Child Well Interactions". SPE-209152-MS

Crespo P., Marcelo Pellicer, Carolina Crovetto, Jorge Gait. "Quantifying the Parent-Child effect in Vaca Muerta Formation", 2020. Unconventional Resources Technology Conference. URTeC-1035

Desjardins P. et al., 2016. Chapter 2 of the book Transecta Regional de la Formación Vaca Muerta.

Suarez M., S. Pichon., 2016. "Completion and Well Spacing Optimization for Horizontal Wells in Pad Development in the Vaca Muerta Shale". SPE-180956-MS